

N 84 - 3 1 3 7 8

**NASA
Technical
Memorandum**

NASA TM-86452

DIELECTRIC CURE MONITORING: Preliminary Studies

By Benjamin E. Goldberg and Marie Louise Semmel
Materials and Processes Laboratory

May 1984



National Aeronautics and
Space Administration

George C. Marshall Space Flight Center

1. REPORT NO. NASA TM-86452		2. GOVERNMENT ACCESSION NO.		3. RECIPIENT'S CATALOG NO.	
4. TITLE AND SUBTITLE Dielectric Cure Monitoring: Preliminary Studies				5. REPORT DATE May 1984	
				6. PERFORMING ORGANIZATION CODE	
7. AUTHOR(S) Benjamin E. Goldberg and Marie Louise Semmel				8. PERFORMING ORGANIZATION REPORT #	
9. PERFORMING ORGANIZATION NAME AND ADDRESS George C. Marshall Space Flight Center Marshall Space Flight Center, Alabama 35812				10. WORK UNIT NO.	
				11. CONTRACT OR GRANT NO.	
12. SPONSORING AGENCY NAME AND ADDRESS National Aeronautics and Space Administration Washington, D.C. 20546				13. TYPE OF REPORT & PERIOD COVERED Technical Memorandum	
				14. SPONSORING AGENCY CODE	
15. SUPPLEMENTARY NOTES Prepared by Materials and Processes Laboratory, Science and Engineering					
16. ABSTRACT <p>Preliminary studies have been conducted on two types of dielectric cure monitoring systems employing both epoxy resins and phenolic composites. An Audrey System was used for 23 cure monitoring runs with very limited success. Nine complete cure monitoring runs have been investigated using a Micromet System. Two additional measurements were performed to investigate the Micromet's sensitivity to water absorption in a post-cure carbon-phenolic material. While further work is needed to determine data significance, the Micromet system appears to show promise as a feedback control device during processing.</p> <p>An additional conductivity related term has been indicated for the dielectric permittivity, ϵ'. This term, heretofore unreported, appears to have significance for high conductivity epoxy and phenolic composites. Previous work on dielectric cure monitoring has always been performed on a parallel plate electrode system; this type of system appears only marginally compatible with epoxy and phenolic composites.</p>					
17. KEY WORDS Cure monitoring; dielectric; epoxy; phenolic; dissipation; polymers; composites			18. DISTRIBUTION STATEMENT Unclassified — Unlimited		
19. SECURITY CLASSIF. (of this report) Unclassified		20. SECURITY CLASSIF. (of this page) Unclassified		21. NO. OF PAGES 37	22. PRICE NTIS

ACKNOWLEDGMENTS

The authors wish to express appreciation to Mrs. Julia Daniels for her assistance during initial Audrey dielectric tests and to Mr. Frank Ledbetter for technical assistance with dynamic mechanical testing presented in this report.

TABLE OF CONTENTS

	Page
INTRODUCTION	1
Background	1
Theory	1
Equipment	9
Materials	9
EXPERIMENTAL PROCEDURES	12
Lay-up Configuration	12
Electrode Fabrication	14
Computer Software	15
Cure Cycles	16
RESULTS AND DISCUSSION	17
Audrey System	17
Micromet System	19
SUMMARY	29
REFERENCES	31

LIST OF ILLUSTRATIONS

Figure	Title	Page
1.	A graphic definition for $\tan \delta = \epsilon'' / \epsilon'$	3
2.	Relationship of ϵ , ϵ' , and ϵ''	5
3.	Cole-Cole plot for single τ	5
4.	Cole-Cole plot for single τ or conductive sample	6
5.	Transitions and responses (ideal)	8
6.	Audrey equipment	10
7.	Micromet equipment.....	11
8.	Lay-up diagram	13
9.	Electrodes	14
10.	Flow chart	15
11.	Cure cycles for phenolic composites.....	16
12.	Audrey II phenolic 3 run	17
13.	Audrey 380 epoxy 2 run.....	19
14.	15-minute epoxy cure.....	20
15.	15-minute epoxy cure.....	20
16.	15-minute epoxy cure.....	20
17.	15-minute epoxy cure.....	20
18.	Room temperature dielectric cure monitoring of Hercules 55A resin ...	22
19.	Highly conductive material phase versus gain responses.....	24
20.	Dielectric responses for phenolic composite material	25
21.	Phase and gain responses for a direct lay-up procedure on phenolic composite material	26
22.	Phase response for indirect lay-up procedure for phenolic composite material	27
23.	Gain response for indirect lay-up procedure for phenolic composite material	27

LIST OF ILLUSTRATIONS (Concluded)

Figure	Title	Page
24.	Loss factor response for indirect lay-up procedure for phenolic composite material	28
25.	Permittivity response for indirect lay-up procedure for phenolic composite material	28
26.	Temperature response for indirect lay-up procedure for phenolic composite material	28
27.	Dynamic mechanical testing of phenolic composite material	30

TECHNICAL MEMORANDUM

DIELECTRIC CURE MONITORING: PRELIMINARY STUDIES

INTRODUCTION

Background

Composite materials are becoming an engineering staple replacing equivalent strength metals while yielding significant weight reductions. Though research on these materials is only 20 years old, it is typically product experience, not scientific knowledge, that governs the material's processing. This evolutionary usage of materials and processes has been a factor in numerous failures of composite structures.

Composites are inherently heterogenous, comprising a matrix material (polymeric or metallic), a reinforcing fiber (polymeric, metallic or ceramic) and, in some cases, a filler. This scope of work centered upon graphite/epoxy and carbon/phenolic materials.

Exotherms from polymerization, cure kinetics, cross-linking reactions, part-specific heat transfer characteristics and hydroclave/autoclave/press temperature profiles/part location will all serve to vary the part temperature from the device temperature. The concerns then are two-fold: First, that the cure process is not optimized for the specific part; second, should the process be tailored, that the entire part will not necessarily see the optimized process temperatures.

The inherent variabilities for these types of cure processes, whether batch-to-batch or within batch, may result in end product property nonuniformity. These types of defects are typically very difficult to isolate with nondestructive tests. Either the part is sacrificed to identify the peculiarities, or used with potentially deleterious results. Clearly, the determination of a methodology to track the part-peculiar parameters is preferred to assure more consistent properties and greater reliability.

The changes in dielectric properties of resin materials undergoing cure processes offer the possibility of tailoring the cure for the specific part geometry for resin variability. Optimization of cure, beginning with process understanding, is vital. These dielectric cure monitoring techniques are currently being evaluated to determine their suitability for carbon-phenolic and filament wound case process optimization.

Theory

While equations are often tedious to follow, it is vital to follow derivation of basic equations to understand the interpretation of cure monitoring results.

The concept of dielectric cure monitoring is, when simplified, quite understandable. Following a treatment by Bottcher, an oscillating electric field:

$$E(t) = E^0 \cos(\omega t) \quad (1)$$

(where E^0 is the amplitude of the imposed field and $\omega = 2\pi \times$ frequency) is imposed on a medium. For any frequency too high for the period of the motions of microscopic particles (10^6 s), the body of the medium acquires a non-zero electric moment; it becomes polarized. The polarization and dielectric displacement will be out of phase with the imposed field.

$$P(t) = P_0 \exp(-t/\tau) \quad (2)$$

$$D(t) = D^0 \cos(\omega t - \delta) \quad (3)$$

(where $P(t)$ = polarization at time t , P_0 = polarization at time 0, τ = a relaxation time, $D(t)$ = dielectric displacement, D^0 = amplitude of a sinusoidal variation, and δ is the phase difference and a function of the frequency). It follows that

$$D(t) = D^0 \cos \delta \cos(\omega t) + D^0 \sin \delta \sin(\omega t) \quad (4)$$

For convenience let

$$\cos \delta (\omega) = \epsilon'(\omega) E^0 / D^0 \quad (5)$$

$$\sin \delta (\omega) = \epsilon''(\omega) E^0 / D^0 \quad (6)$$

Then $D(t)$ may be written as

$$D(t) = \epsilon'(\omega) E^0 \cos(\omega t) + \epsilon''(\omega) E^0 \sin(\omega t) \quad (7)$$

It is from this form of $D(t)$ that $\epsilon'(\omega)$ and $\epsilon''(\omega)$ are specified. Consider that, as

$$D(t) \equiv \epsilon E(t) \quad (8)$$

(where ϵ is the dielectric constant) then

$$D(0) = \epsilon'(0) E^0 + \epsilon''(0) E^0(0) = \epsilon'(0) E^0$$

for a frequency of 0.

Then $\epsilon'(\omega)$ is defined as the frequency dependent dielectric constant or the permittivity. $\epsilon''(\omega)$ is a measure of the amplitude of the component of $D(t)$ 90 deg out of phase with $E(t)$ — $E(t)$ is a cosine term while $\epsilon''(\omega)$ represents a sine term. $\epsilon''(\omega)$ is defined as the loss factor.

Other terms used commonly for dielectric monitoring include $\tan\delta$ and gain. $\tan\delta$ is defined as the tangent of the angle between the real and imaginary components of the dielectric constant (Fig. 1). Using complex notation the imposed electric field may be written as

$$E(t) = E^0 e^{i\omega t} = E^0 \cos(\omega t) + i E^0 \sin(\omega t) \quad (9)$$

and

$$D(t) = D^0 e^{i(\omega t - \delta)} \quad (10)$$

This leads to

$$D^0 = E^0 (\epsilon'^2 + \epsilon''^2)^{\frac{1}{2}} \quad (11)$$

and

$$\tan\delta = \epsilon''/\epsilon' \quad (12)$$

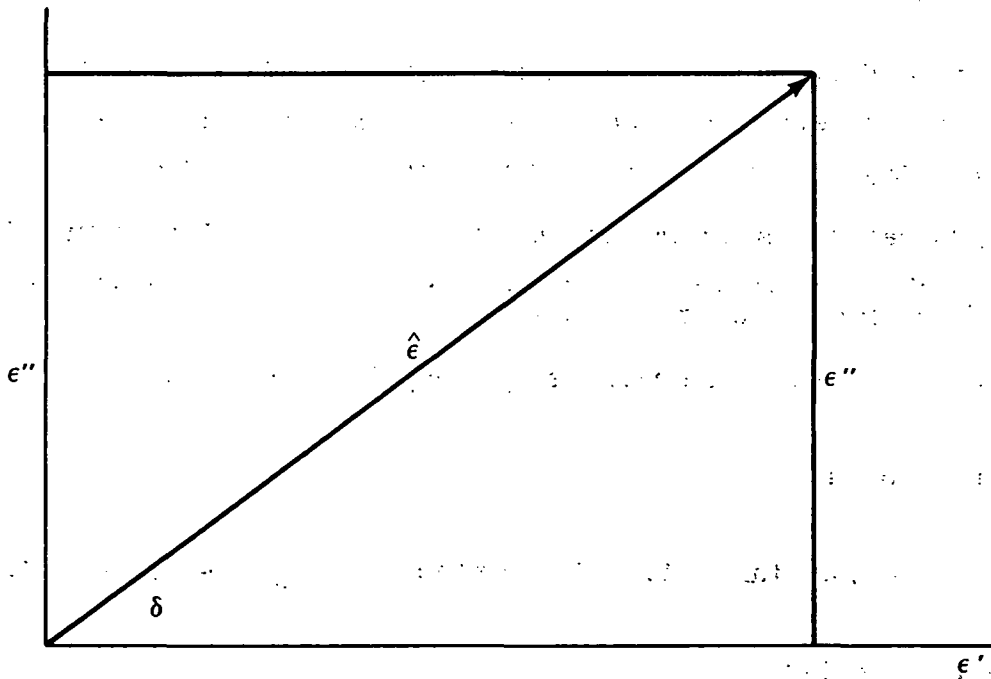


Figure 1. A graphic definition for $\tan\delta = \epsilon''/\epsilon'$. The $\tan\delta$ should be geometry independent.

Equations (11) and (12) may be derived; however, that is beyond the scope of this report. It follows from equations (9), (10), and (8) that

$$\hat{E}(\omega) = \frac{D^0}{E^0} e^{-i\delta} \quad (13)$$

which leads to

$$\hat{D}(t) = \hat{\epsilon}(\omega) \hat{E}(t) \quad (14)$$

The correspondence of the complex terms may be completed by combining equations (7), (9), and (14) to find

$$\hat{\epsilon}(\omega) = \epsilon'(\omega) - i\epsilon''(\omega) \quad (15)$$

To this point all equations have been for an ideal system that behaves with a singular relaxation time for all responses. These assumptions are continued for the derivation of the Debye equations:

$$\epsilon'(\omega) = \epsilon_{\infty} + (\epsilon_0 - \epsilon_{\infty}) / (1 + \omega^2 \tau^2) \quad (16)$$

$$\epsilon''(\omega) = (\epsilon_0 - \epsilon_{\infty}) \omega \tau / (1 + \omega^2 \tau^2) \quad (17)$$

(where ϵ_{∞} may be viewed as the unrelaxed orientation dielectric constant, or the permittivity at a frequency $\gg \tau^{-1}$ and ϵ_0 as the relaxed orientation, or the permittivity at a frequency $\ll \tau^{-1}$; τ is the relaxation time of the system.)

$\epsilon_0 - \epsilon_{\infty}$ is defined as the relaxation strength of the dielectric and $\epsilon''(\omega)$ may be seen to be a maximum at $\omega = 1/\tau$ (Fig. 2). This is why certain frequencies will display specific reactions during the cure cycle [1].

Assuming that relaxation processes typically follow an Arrhenius equation, let

$$\tau = A \exp(\Delta H^*/RT) \quad (18)$$

thus displaying a temperature effect [2]. Setting $\omega = \omega_{\max}$, equation (17) indicates

$$\epsilon'_{\max} = (\epsilon_0 - \epsilon_{\infty})/2 \quad (19)$$

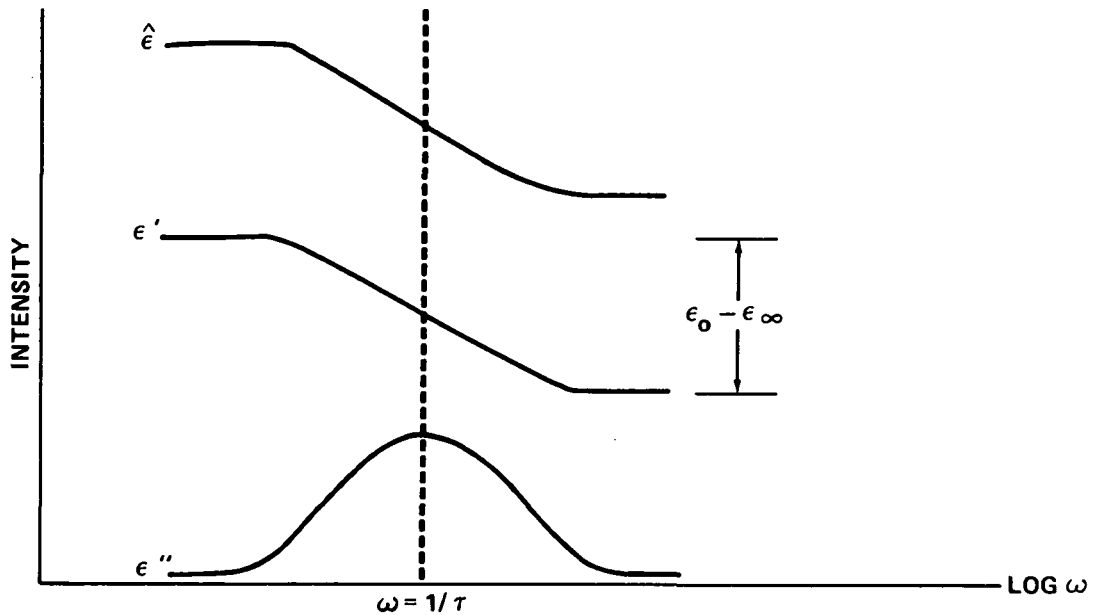


Figure 2. Relationship of $\hat{\epsilon}$, ϵ' , and ϵ'' . Note that ϵ''_{\max} occurs at $\epsilon_0 - \epsilon_\infty / 2$.

as $\omega_{\max} = 1/\tau$. Equation (19) is used in the Cole-Cole relationship

$$\left(\epsilon' - \frac{(\epsilon_0 - \epsilon_\infty)}{2} \right)^2 + \epsilon''^2 = \frac{(\epsilon_0 - \epsilon_\infty)^2}{4} \quad (20)$$

which is clearly the equation of a circle. ϵ'' is plotted versus ϵ' and, for a singular τ (relaxation time) is a semicircle with ϵ_0 and ϵ_∞ the maximum and minimum ϵ' values (Fig. 3). Other relationships, most notably Cole-Davidson, attempt to encompass a distribution of relaxation times for a given system. However, with highly conductive systems, the empirical data deviates widely from the idealized theory (Fig. 4).

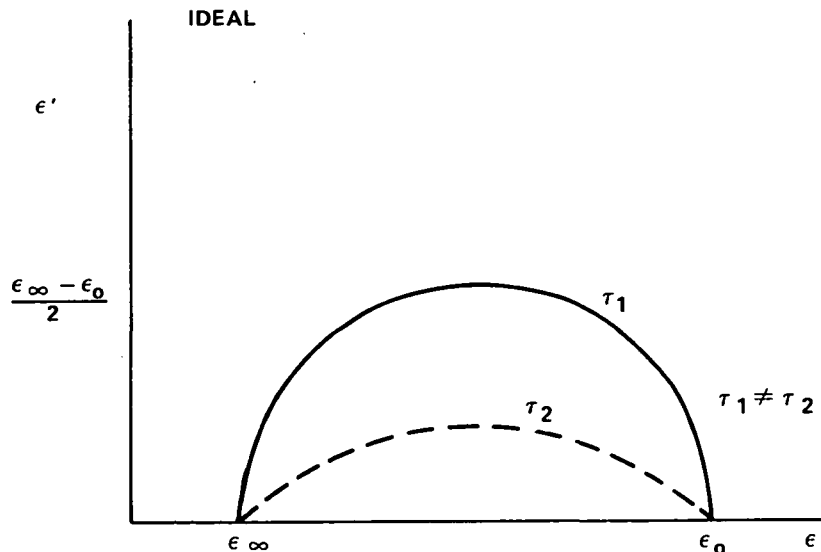


Figure 3. Cole-Cole plot for single τ .

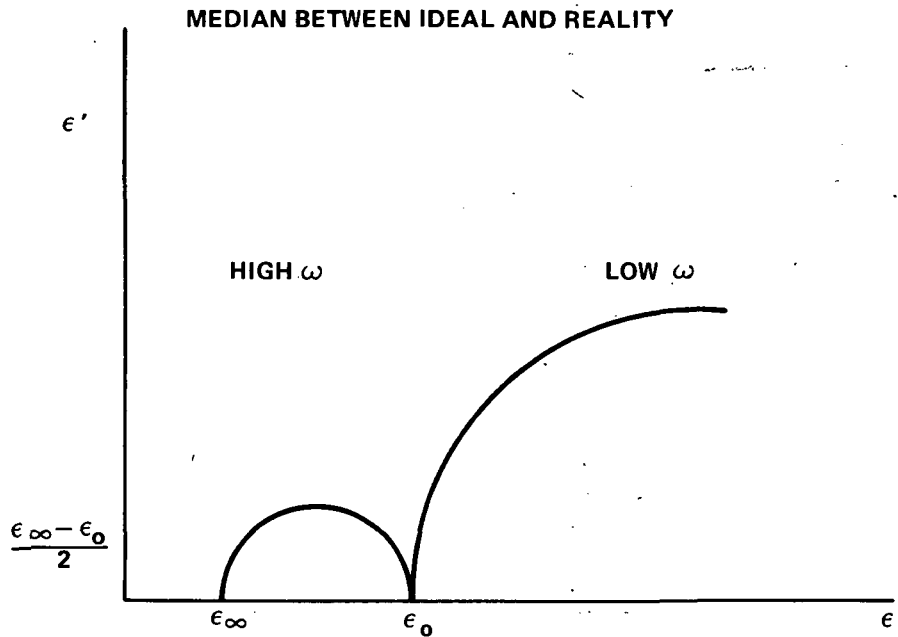


Figure 4. Cole-Cole plot for single τ or conductive sample. For a distribution of relaxation times (reality) the semi-circles are skewed.

Cole-Davidson

$$\frac{\hat{\epsilon} - \epsilon_{\infty}}{\epsilon_0 - \epsilon_{\infty}} = \frac{1}{(1 + i\omega\tau)^2} \quad (21)$$

Havriliak-Nagami

$$\frac{\hat{\epsilon} - \epsilon_{\infty}}{\epsilon_0 - \epsilon_{\infty}} = \frac{1}{(1 + (i\omega\tau)^{1-\alpha})^{\beta}} \quad (22)$$

Equations (21) and (22) are standard dielectric equations for plotting and interpreting data; α and β are empirically defined curve fitting constants. Again, while these equations add a distribution of relaxation times to the ideal theory, they do not fit for highly conductive systems.

For a conductive medium

$$\epsilon'' = \epsilon''_{\text{dielectric loss factor}} + \epsilon''_{\text{loss due to conductivity}} \quad (23)$$

where $\epsilon''_{\text{dielectric loss factor}}$ is defined as in equation (17) and $\epsilon''_{\text{loss due to conductivity}} = (\sigma/\omega)$, (σ = bulk conductivity) [3].

No such additional conductivity term may be found in the literature for ϵ' . For a system with very small distances between the dielectric plates — as is the case for microdielectric monitoring — an additional term is needed. Boundary layer effects due to ionic buildup, and subsequent shielding of the electrodes, indicate the term should be diffusion controlled.

$$\epsilon' = \epsilon_{\infty} + (\epsilon_0 - \epsilon_{\infty}) / (1 + (\omega\tau)) + \epsilon'_{\text{ionic conduction}} \quad (24)$$

One possible, over-simplified, term may be derived from

$$\epsilon' \equiv \frac{C_x}{C_0} = \frac{D(t)}{E(t)} \quad (25)$$

(where C_x = capacitance of dielectric medium, C_0 = capacitance for space filled with vacuum). Ion concentration may be characterized:

$$J = \sigma E(t) = E(t) / \rho = c(e) \mu E(t) = c(e)v \quad (26)$$

(where J = current density and ρ = resistivity, μ = ion mobility, e = electron charge, c = ion concentration, and v = ion drift velocity) [4]. As the diffusion constant, (D) may be defined by

$$D = \mu kT/e \quad (26)$$

(where k = Boltzmann constant and T = temperature), it follows from equations (25), (26), and (27) that

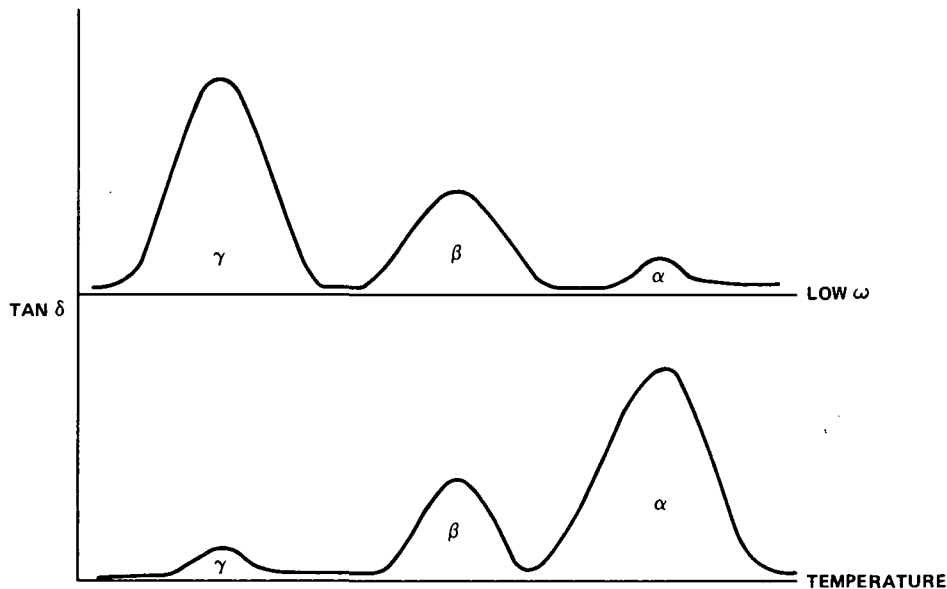
$$\epsilon'_{\text{ionic conduction}} = \frac{D(t)D e}{v k T} \quad (28)$$

The above equations serve to illustrate the electrical parameters that are monitored during cure monitoring. Five major types of events may be monitored by this technique:

- (1) electron displacement
- (2) ionic displacement
- (3) dipole or orientational polarization
- (4) translational polarization
- (5) macroscopic polarization

Electron displacement is manifested by a shift in the electron clouds such that they oscillate with the imposed field. From a physical standpoint, this is the smallest motion (excluding phonon interaction). Ionic displacement is only observed in molecules with heteropolar bonds. Dipole or orientational polarization represents the motion of the dipolar moieties due to the imposed field. The competition between the orienting action of the field and the disorienting action of thermal motion leads to a time dependence for the orientational polarization. Translational polarization (ion transfer) and macroscopic polarization — the formation of charged layers at the interfaces in heterogeneous materials — fill out the field of polarization mechanisms [5].

Dielectric monitoring will also define flow, α or glass transition regions where 10-50 backbone carbon atoms acquire mobility, β transitions where a crankshaft rotation of two repeat units takes place and the previously explained γ or dipolar motion where no backbone motion takes place (Fig. 5).



- α = GLASS TRANSITION REGION (10-50 BACKBONE CARBON ATOMS ACQUIRE MOBILITY).
- β = TRANSITION REGION WHERE A CRANKSHAFT ROTATION OF TWO REPEAT UNITS TAKE PLACE
- γ = TRANSITION REGION FOR MOTION OF DIPOLAR MOIETIES; NO BACKBONE MOTION TAKES PLACE.

Figure 5. Transitions and responses (ideal).

During the cure cycle of a phenolic, all of the above polarizations and transitions take place. A large distribution of relaxation times, high conductivity of the resin system and second phase fiber heterogeneities further complicate the process. Consider, the complication induced by a second phase heterogeneity for an ideal situation may be defined by

$$\tau = [(n-1) \epsilon'_1 + \epsilon'_2] / 4\pi k_2 \tag{29}$$

(where the subscripts 1 and 2 reflect the phases, k is the conductance and n is a geometric factor). The τ defined is a singular relaxation time. The situation is still further complicated by the extremely high conductivity which not only adds additional terms to the dielectric equations, but which masks the responses of the matrix, preventing their detection.

A dielectrometer is used to obtain the empirical data predicted by theory. This unit is typically a capacitance bridge specifically designed for low frequency, low signal applications. Six monitorial properties may be examined during a cure cycle: ϵ' (permittivity), ϵ'' (loss factor), phase, gain, dissipation ($\tan\delta$) and capacitance. In addition, temperature and pressure versus time are recorded to correlate cure events with process conditions.

Equipment

Earliest work was done with an Audrey II, an automatic dielectrometer which is manually set to a single frequency between 100 Hz and 1000 Hz. The outputs from this unit (temperature, dissipation, and capacitance) were fed to strip chart recorders.

The Audrey II was subsequently replaced by an Audrey 380 system with single, sweep and step capabilities between 100 Hz and 100 KHz. This Audrey has been interfaced to a Hewlett-Packard 3054-A Data Acquisition System, providing the capacity to monitor up to five frequencies at a time. The computer stores the Audrey outputs (frequency, loss factor, capacitance, dissipation, temperature) and allows plotting of the data in any combination (Fig. 6).

In addition to the Audrey system, a monoprobe dielectrometer (Micromet System II) was investigated. The Micromet has a frequency range from 0.02 Hz to 20 KHz and measures loss factor, permittivity, phase, gain and temperature directly from the small (2 mm x 3 mm) monoprobe sensor. These signals from the sensor go to the Fourier Transform Signal Analyzer and are then sent to a Hewlett-Packard HP85-B microcomputer for manipulation, output, and storage (Fig. 7).

Materials

Initial emphasis has been on SRM nozzle material. This material, available from Fiberite as MX4926 and U.S. Polymeric as FM5055, is carbon cloth impregnated with a phenolic resin and carbon filler. In addition to tests on the prepreg, tests were run on extracted phenolic resin.

As a secondary activity, work is proceeding on the Filament Wound Case material, which utilizes both Hercules 55A epoxy resin and Hercules 3501 epoxy resin with AS-4 graphite fiber. As preliminary studies, runs have been made on Shell 828 epoxy resin with Z activator and on Fiberite 1034 prepreg tape. The prepreg is AS-4 fiber with Fiberite 934 epoxy resin.

As part of the initial system check and performance evaluation for the Micromet System II, runs were made on two fast curing epoxies; Hysol Epoxi-patch Kit 608 clear (a 15-minute epoxy) and Hysol Epoxi-patch Kit 1C white (a 30-minute epoxy).

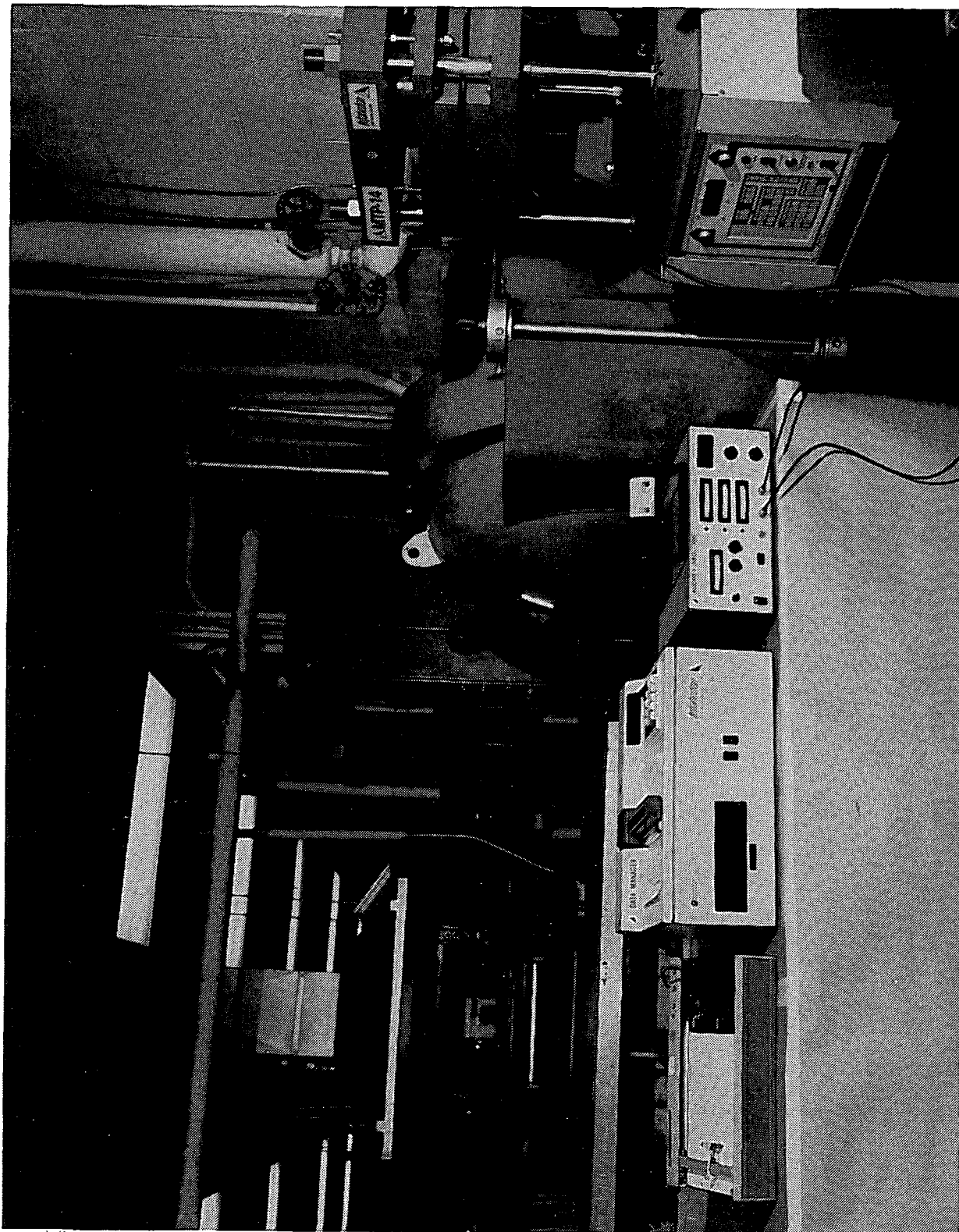


Figure 6. Audrey equipment.

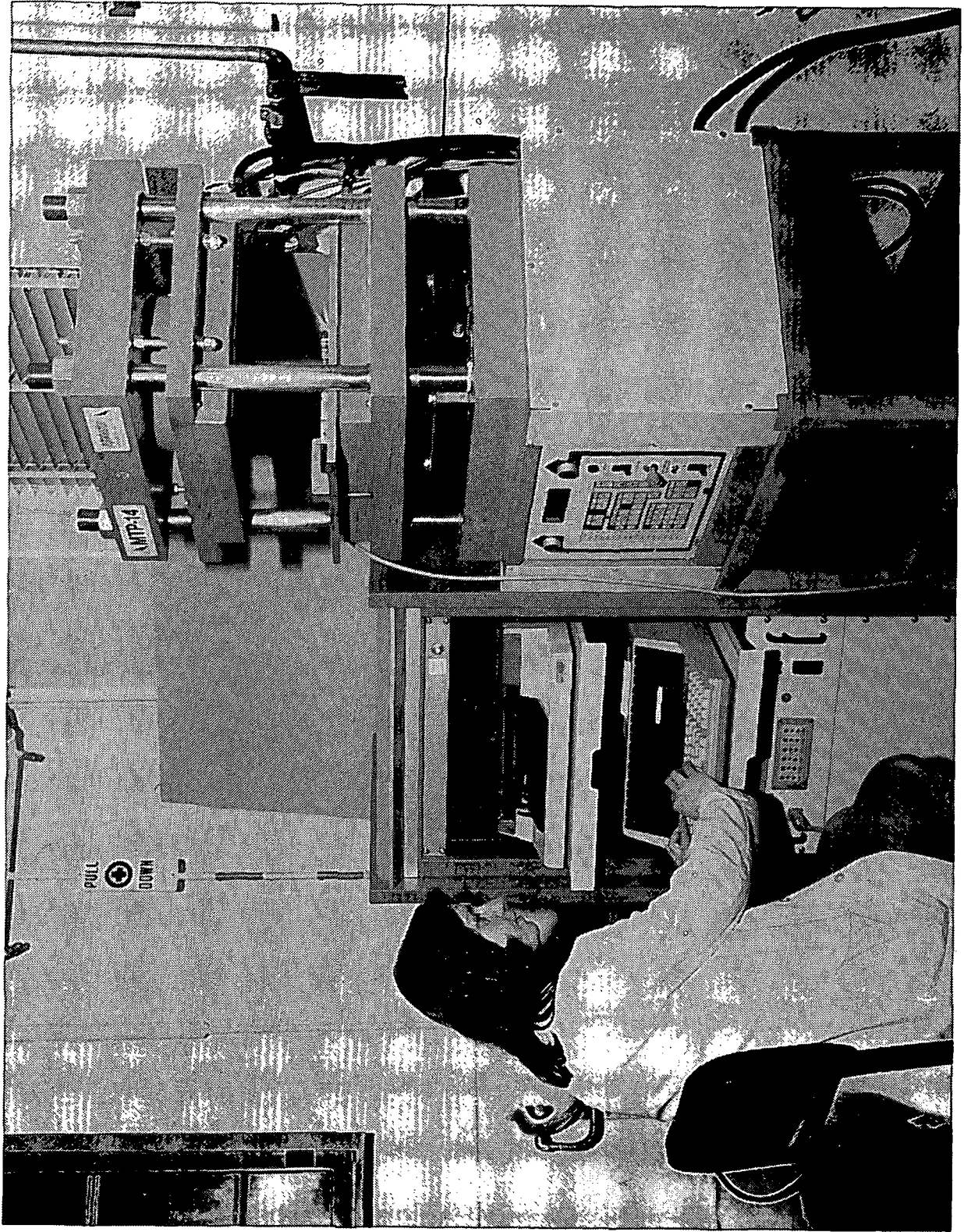


Figure 7. Micromet equipment.

EXPERIMENTAL PROCEDURES

Experimental procedures may be divided into four major categories: configuration, electrode fabrication, computer software, and cure cycles.

Lay-up Configuration

Four types of lay-up procedures were utilized during this investigation — two for the Audrey system, two for the Micromet system:

Audrey 1 (direct method) (Fig. 8)

bottom platen coated with teflon
kapton insulation layer
teflon coated fiberglass breather
electrode
carbon-prepreg (2 to 3 plies)
electrode
teflon coated fiberglass breather cloth
paper bleeder cloth
teflon coated fiberglass breather cloth
top platen

Audrey 2 (indirect method)

bottom platen coated with teflon
kapton insulation layer
teflon coated fiberglass breather
carbon-prepreg
electrode
paper bleeder cloth
electrode
carbon-prepreg
teflon coated fiberglass breather cloth
paper bleeder cloth
teflon coated fiberglass breather cloth
top platen

Micromet 1

kapton layer
teflon coated fiberglass breather
paper bleeder cloth
carbon prepreg - 2 layers
carbon prepreg - 3 layers with slits cut out where the monoprobe is
inserted
carbon prepreg - 2 layers
paper bleeder cloth
teflon coated fiberglass breather
kapton layer

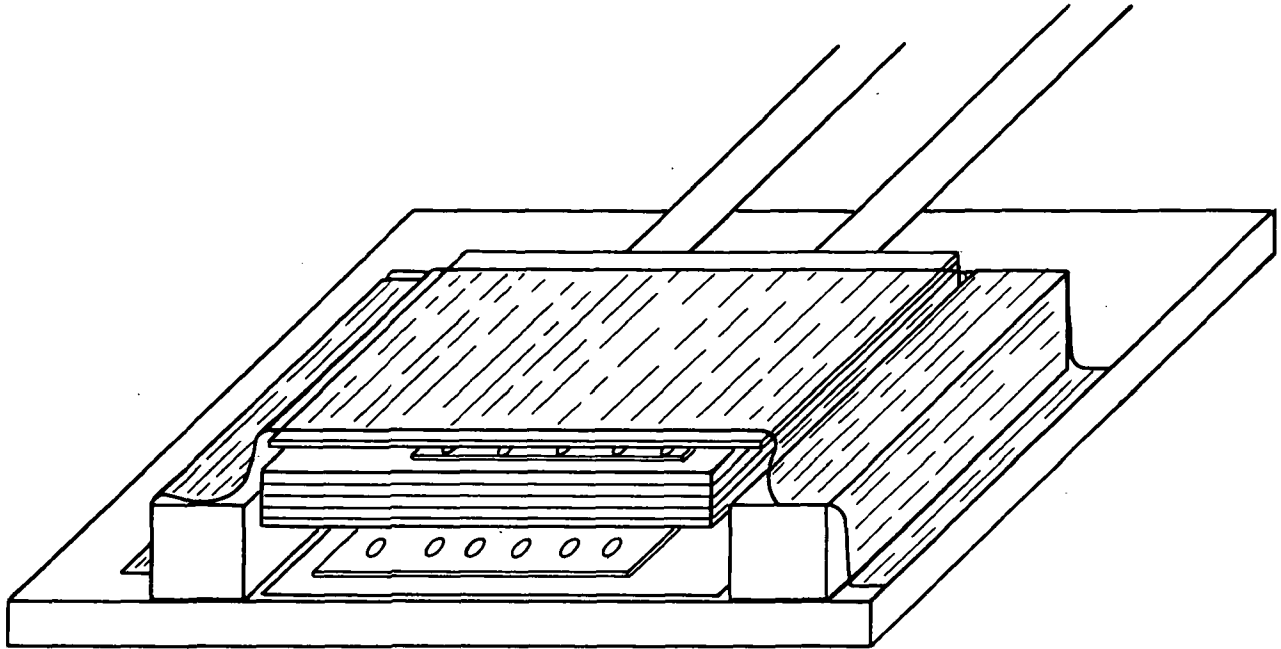


Figure 8. Lay-up diagram featuring cork dam, bottom platen, teflon sheet, teflon coated fiberglass, electrode - coated and punched, prepreg material, electrode - coated and punched, bleeder layer, top platen, vacuum bag. (Variations on this lay-up procedure include electrode changes (to copper coils or microchip monoprobe types), vacuum bag removal, and thermocouple insertion. The cork dam surrounds the entire stack, not just the two sides pictured in the cut-away view.)

Micromet 2

bottom platen coated with teflon
 teflon coated fiberglass breather
 carbon prepreg - 3 layers with slits cut out where the monoprobe is inserted
 carbon prepreg - 2 layers
 teflon coated fiberglass breather cloth
 paper bleeder cloth
 teflon coated fiberglass breather cloth
 nylon coated top platen

The lay-ups were typically vacuum bagged and a cork dam constructed around the lay-up stack. The Audrey lay-ups also included two thermocouples implanted in the lay-up stack, away from the electrodes. Some of the Audrey runs also had a differential thermocouple in the lay-up - one probe in the lay-up stack, the other resting on a second lay-up stack consisting of:

bottom platen used for entire assembly
 viton rubber sponge material
 post-cured carbon composite 2 in. x 2 in. square
 differential thermocouple probe
 teflon coated fiberglass breather
 paper bleeder cloth
 teflon coated fiberglass breather
 top platen

Electrode Fabrication

Four types of electrodes were fabricated — three from a basic aluminum foil square design and one coil design (Fig. 9):

Solid bare square — This design is a 2 in. x 2 in. square of 0.003 in. aluminum foil with a 9 in. tail for electrical connections.

Perforated bare square — A punched version (10-3/16 in. diameter holes) of the solid bare square.

Coated perforated square — The perforated bare square is coated with GE Glyptal 1202 or with nylon tape. When nylon tape is used, it is punched to match the perforations on the electrode.

Coated copper coils — Coated copper wire (No. 26 transformer wire) is wound on a cone-shaped mandrel and pressed flat for use.

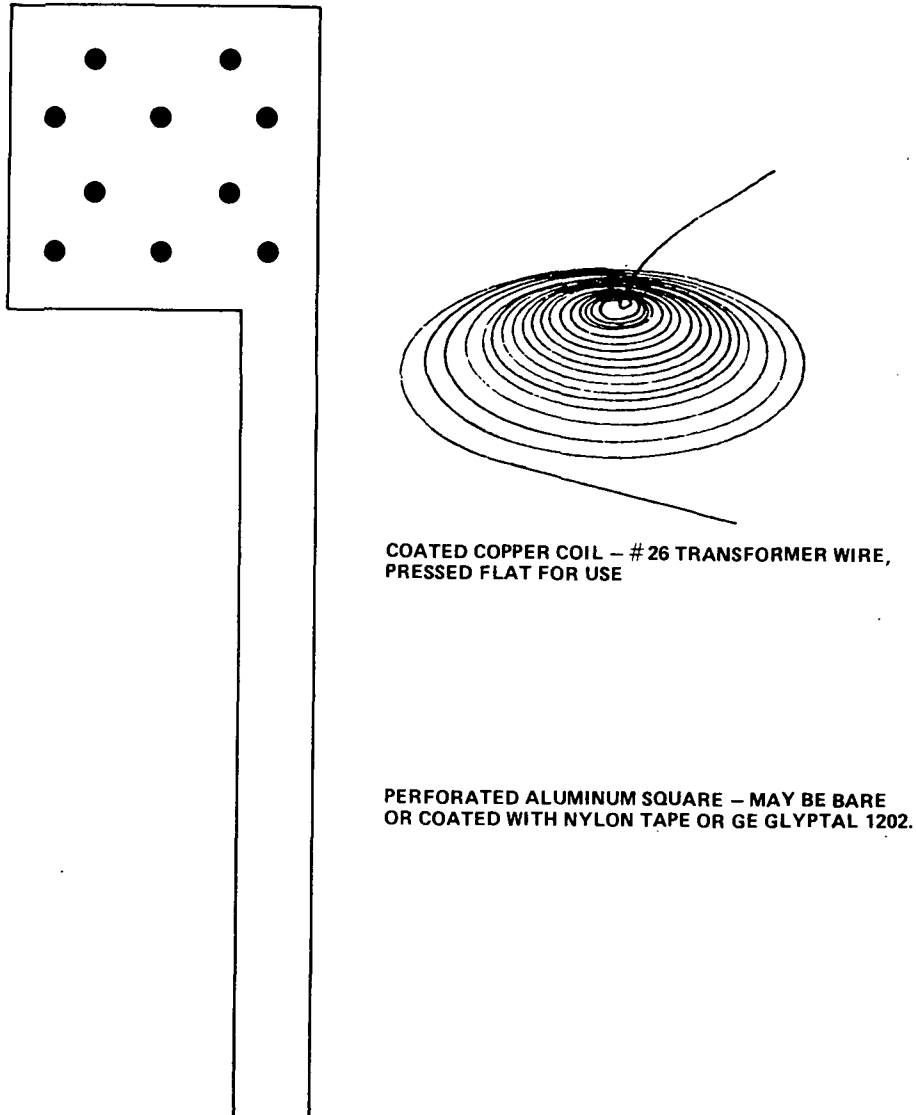


Figure 9. Electrodes.

Computer Software

Two types of software were used. The software used by Micromet System II is supplied by the manufacturer; therefore, only the software developed in-house for the Audrey will be discussed.

The overriding factor in the design of the data acquisition program was the lack of a digital/analog converter with which to control the Audrey. Therefore, the program is passive and inefficient. The Audrey sweeps through the desired frequency range, while the computer waits for preset frequencies to take data (Fig. 10).

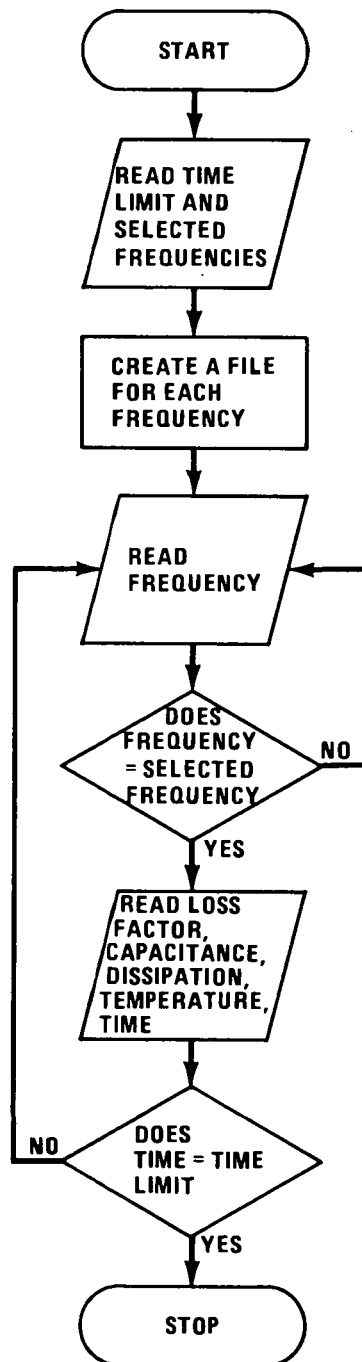


Figure 10. Flow chart.

Cure Cycles

Five cure cycles were monitored during this investigation — two for epoxy resins and three for phenolics:

Epoxy 1 — temperature ramp to 160°F

Epoxy 2 —

- 1) apply vacuum for 30 minutes to debulk
- 2) maintaining vacuum, raise temperature to 250°F (+5 -10°F) at 2-5°F per minute under touch pressure
- 3) hold at 250°F (+5 -10°F) for 15 ± 5 minutes
- 4) apply 100 (+5 -0) psi pressure
- 5) hold at 250°F (+5 -10°F) and 100 (+5 -0) psi for 45 ± 5 minutes
- 6) raise temperature to 350°F (+10 -0°F) at 2-5°F per minute
- 7) hold at 350°F (+10 -0°F) for 2 hours ± 15 minutes
- 8) cool under pressure and vacuum to below 175°F

Phenolic 1 — temperature ramp to 310°F

Phenolic 2 — see Figure 11 old

Phenolic 3 — see Figure 11 new

As cure monitoring development was of major interest, the majority of the monitored runs ended at the cooling regime.

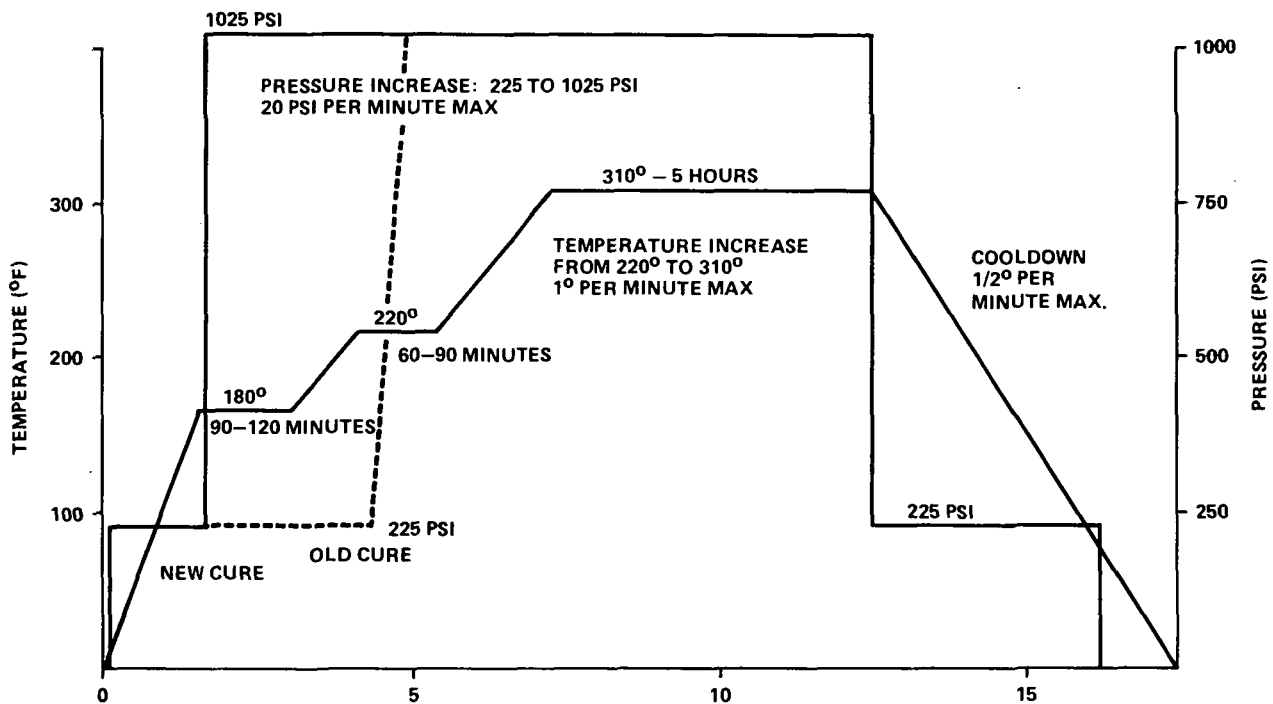


Figure 11. Cure cycles for phenolic composites. The only difference between old and new cure cycles is the time (and temperature) of the pressure rise from 225 to 1025 psi.

RESULTS AND DISCUSSION

The results of the investigation may be divided into two major categories: Audrey System results and Micromet microdielectrometer results. The two systems, while measuring the same types of responses, differ fundamentally. The Audrey system employs two parallel plate electrodes, closely spaced, to input an oscillating electric field and measure the response of the dielectric medium between the plates. The capacitance of the system is proportional to the dielectric permittivity (ϵ'). The calibration of the system is dependent upon the system geometry — both the area and spacing of the plates. During the cure cycle, resin flow and expansion can change plate spacing. As a result, the loss tangent (ϵ''/ϵ') is monitored rather than ϵ' or ϵ'' ; the theory being that, while ϵ'' and ϵ' will both be affected by plate spacing, the loss tangent is geometrically independent.

The Micromet microdielectrometer system has electrodes based on an integrated circuit with fixed geometry. This system requires significant amplification; however, when implanted in the resin or composite during cure, the system is geometrically independent. ϵ' , ϵ'' , gain, phase and $\tan\delta$ may all be monitored. A further advantage of the system is an effective thermocouple located in the integrated circuit microchip which monitors temperature at the site of the dielectrically monitored area.

Audrey System

Nine complete monitoring runs were investigated using the Audrey II system after a comparable series of start-up tests. Five of these runs included differential thermal analysis (DTA) capability. While the DTA technique showed promise, no significant data was extracted from these tests (Fig. 12).

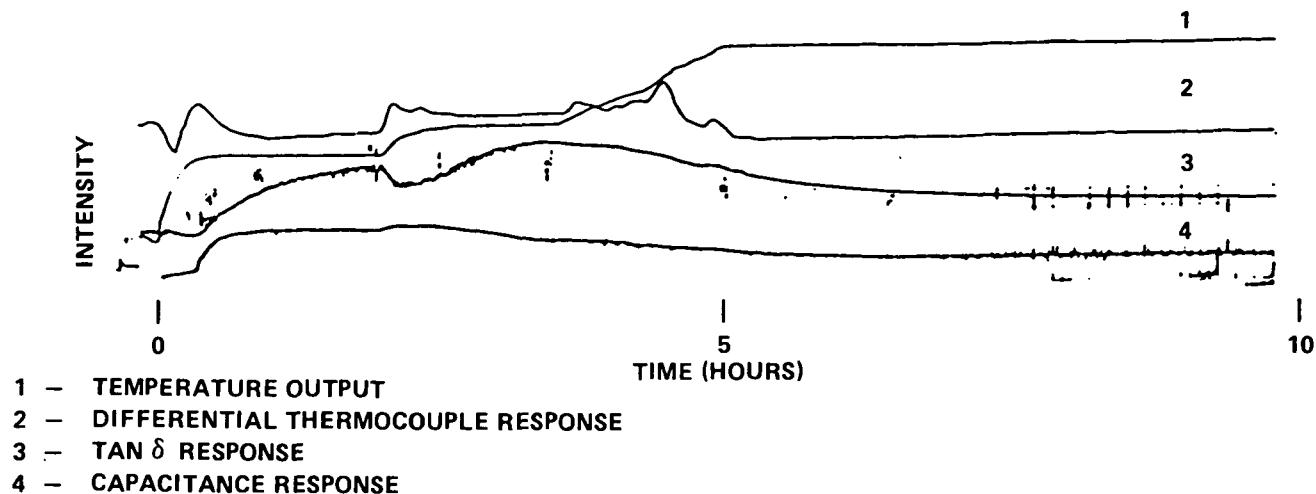


Figure 12. Audrey II phenolic 3 run.

Fourteen complete monitoring runs were investigated using the Audrey 380 system in an attempt to determine the system's capabilities and resin-specific applicabilities. Eleven of the Audrey 380 runs were epoxy materials, the remaining three were phenolics. No differential temperature monitoring was attempted.

The Audrey systems require two electrodes as parallel plates with the sample as the dielectric medium of the capacitive cell. Electrodes may be almost any material through which an electrical signal can be passed. Earliest experiments were conducted with aluminum foil squares. This configuration proved unsatisfactory for the indirect lay-up, so the squares were perforated to allow better resin flow into the area between the electrodes. As evidence mounted that the bare foil electrodes were being shorted out by the highly conductive carbon/phenolic, various methods of shielding the electrodes were tried. All involved placing a physical barrier between the resin and the electrodes. Nylon tape and GE Glyptal 1202 proved to be opaque to the dielectric signal.

The inherent difficulties of the foil square necessitated a second electrode design: coiled coated copper wire. This coated copper wire (transformer wire) was wound on a cone-shaped mandrel and then pressed flat.

For resin samples, the compression test cell can serve as the electrode pair. This test cell is a self-contained unit consisting of a non-conductive cup and cover with embedded electrodes. The cell is inserted between the platens of a conventional press for clamping pressure and heat.

The epoxy material runs may be divided both by electrode coatings and lay-up configuration:

<u>Run Number(s)</u>	<u>Cure Cycle</u>	<u>Electrode Coating</u>	<u>Comments</u>
1 _{indirect soaked bleeder}	Epoxy 1	bare	Saw relaxation peaks, both capacitance and dissipation displayed frequency dependency.
2 _{indirect lay-up}	Epoxy 2	bare	Saw relaxation peaks, both capacitance and dissipation displayed frequency dependency (Fig. 13).
3-6 _{direct lay-up}	Epoxy 2	nylon tape	Attempts to shield electrodes to prevent DC leakage and subsequent masking of relaxation phenomena. Little signal penetration of electrode coating.
7 _{indirect lay-up}	Epoxy 2	Glyptal 1202	Attempts to shield electrodes to prevent DC leakage and subsequent masking of relaxation phenomena. Little signal penetration of electrode coating.
8-10 _{direct and indirect}	Epoxy 2	copper coils	All coils developed shorts indicating the copper coating could not withstand cure cycle conditions.
11-12	Phenolic 1	compression test cell	Initial attempts to determine compression test cell methodology for phenolic prepreg. No significant data.

<u>Run Number(s)</u>	<u>Cure Cycle</u>	<u>Electrode Coating</u>	<u>Comments</u>
13	Epoxy 2	Compression test cell	Initial attempt to determine compression test cell methodology for epoxy prepreg. No significant data.
14 resin soaked bleeder	Phenolic 2	bare	Attempt to use procedure developed in Run (1) for phenolic resin extracted from prepreg. No significant data.

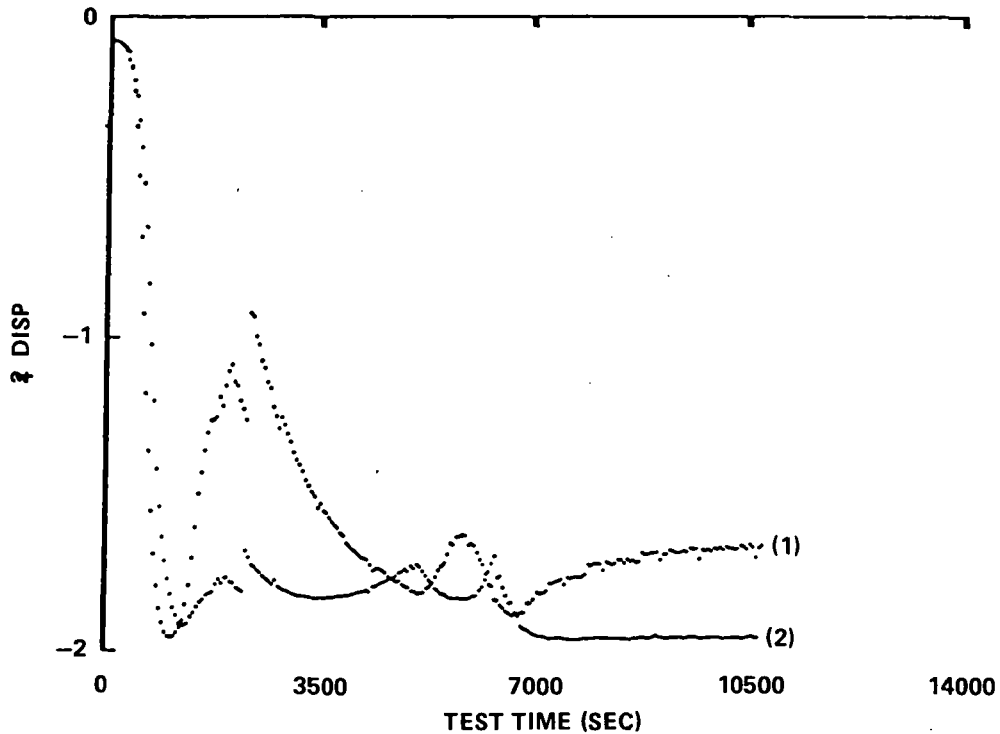


Figure 13. Audrey 380 epoxy 2 run.

A review of the presented results indicates that the Audrey System has basic incompatibilities with highly conductive, heterogeneous composite materials. While successful results were obtained for epoxy resin in an indirect lay-up configuration, this method is not suitable in a feed-back cycle for process control. The bare electrodes used for this lay-up configuration (indirect) are incompatible for the direct lay-up configuration necessary for a feedback interactive system. The investigation of other, less dielectrically opaque coatings is continuing; however, to date there are no indications that the Audrey system will be found compatible as a feedback device for a production facility.

Micromet System

Nine complete cure monitoring runs were investigated using the Micromet System II Microdielectrometer. Two additional measurements were performed to investigate the Micromet's sensitivity to water absorption in a post-cure carbon-phenolic material.

Two of the Micromet runs were on epoxy materials, Hysol 608 clear, 15-minute and Hysol 1C white, 30-minute resins. The two part epoxy system was mixed and a globule placed on the monoprobe. The curing of the epoxies was monitored by both dielectric and thermal responses (Figs. 14, 15, and 16). The phase versus gain plot for the 15-minute epoxy is instructive in that it displays three distinct regions (Fig. 17).

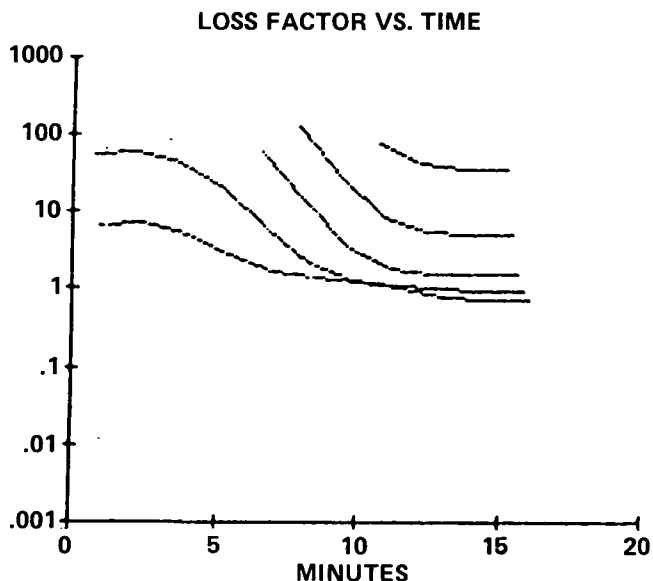


Figure 14. 15-minute epoxy cure.

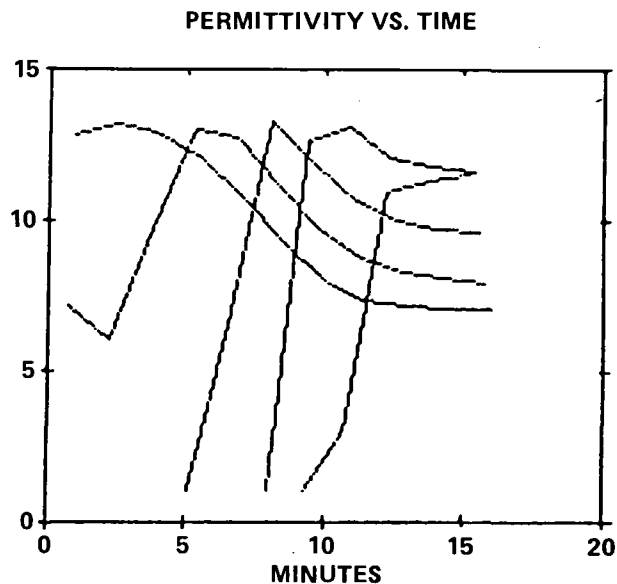


Figure 15. 15-minute epoxy cure.

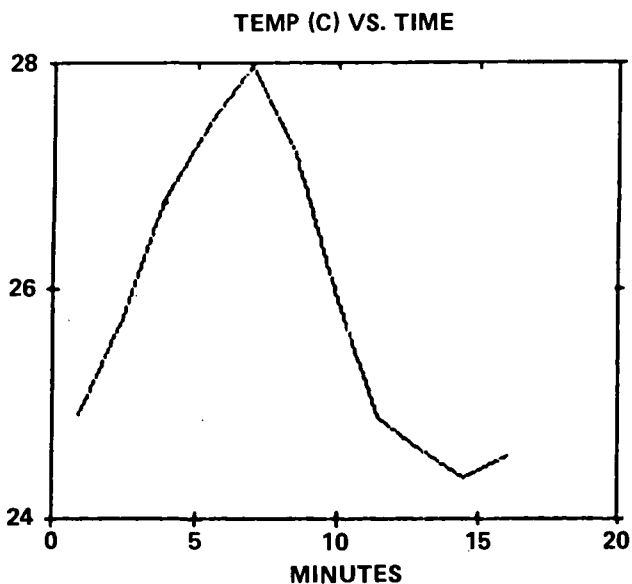


Figure 16. 15-minute epoxy cure.

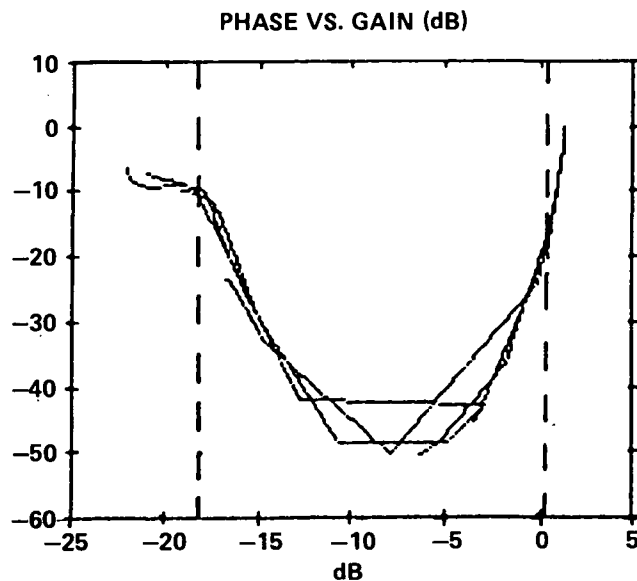


Figure 17. 15-minute epoxy cure.

Note the correlation of slope deviation regions for Figures 14 through 17. The permittivity versus time display reveals the frequency dependence of the transitions.

(1) The initial point of the cure cycle where the values of phase and gain both approach 0. The epoxy moieties are in phase with the imposed field — the system behaves as an electrical short. As the system cures, the resin hardens and the dielectric responses become farther out of phase with the imposed field.

(2) The crosslinking of the epoxy resin ends and the phase lag of the epoxy moieties moves toward 0. The system is not shorting; however, the amplitude remains significantly off 0, indicating that, while the system is "frozen" and no longer able to react with the imposed field and generate heat, its capacitance differs significantly from that of C_0 .

(3) This final portion of the curve indicates that the previous regions were dominated by boundary layer ionic conduction effects. The system has lost the highly conductive polar solvent system and has become less conductive. The ionic interference is minimized.

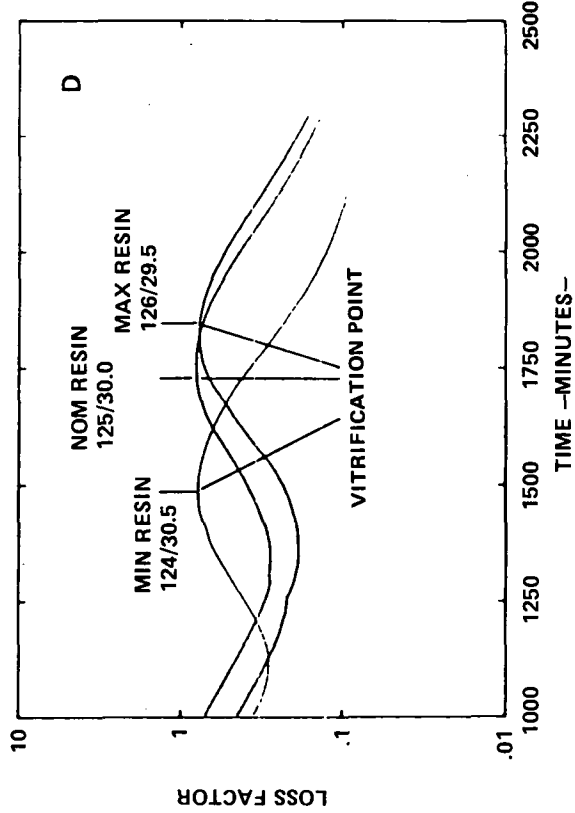
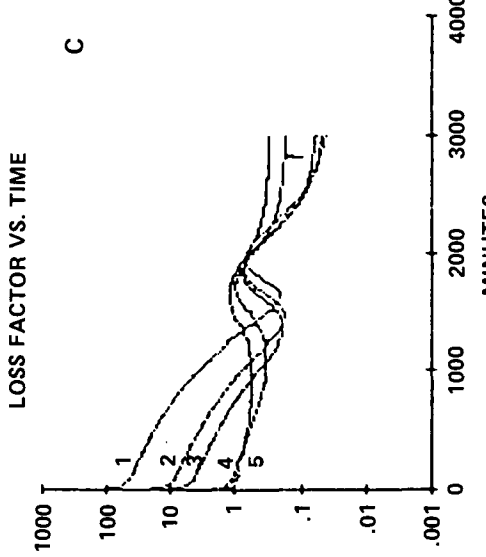
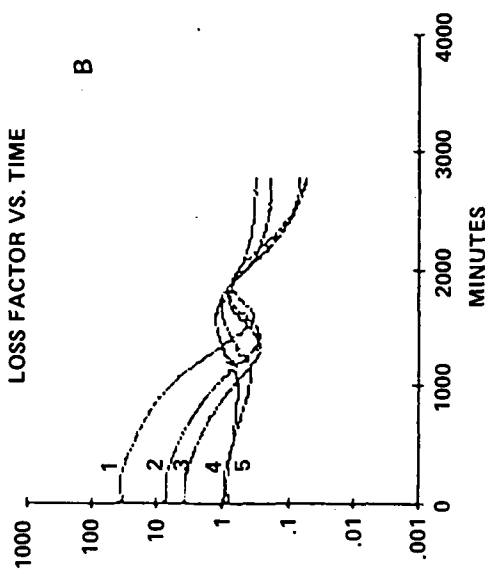
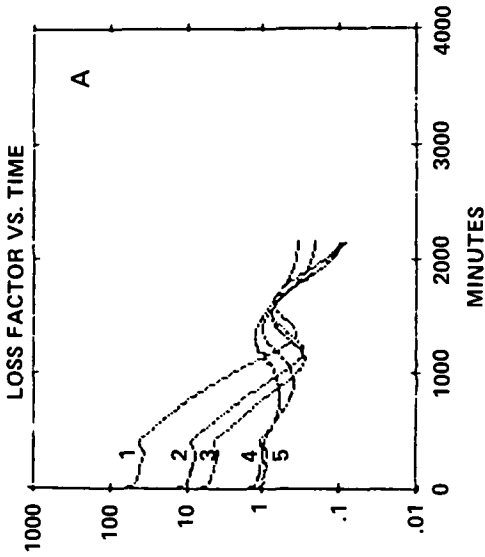
Three cure monitoring runs were performed on another epoxy resin system — Hercules 55A. These runs investigated the effects of the catalyst to resin ratio on cure transition events during a room temperature cure cycle. Three different catalyst to resin mixtures were investigated to span the extremes allowed by the specifications: 30.5/124, 30/125, 29.5/126 (weight percents) (Fig. 18). Gellation regions are evident for all traces and all frequencies. Mechanical data, used to corroborate the study, indicated the region at the apex of the vitrification peak corresponded to a vitrification point. As expected, the largest catalyst to resin ratio mixture cured in the least time. Vitrification points of 24.6 hours, 28.3 hours and 30.8 hours were defined at 1 KHz for ratios of 30.5/124, 30/125, and 19.5/126 respectively. The 1 KHz data was chosen as representative in defining catalytic effects.

Two measurements were performed on cured phenolic composite systems to determine water absorption. The samples were tested at seven frequencies for ϵ' and ϵ'' responses then placed in a vacuum oven for 1 hour at 50°C. The samples were then retested to determine changes. While the results vary considerably for the two samples, PHEN1, the first to be retested after removal from the oven, displays significant gains in permittivity and loss factor — gains expected due to removal of water boundary layers (Table 1). It is possible that PHEN2 picked up enough water during the time after removal from the oven and before testing, to recreate the boundary layer effects. While the significance of the data is questionable, further testing along these lines is clearly warranted.

Four measurements were performed on curing phenolic composite systems (Table 2); two measurements were for temperature ramps, two for a full cure cycle (new):

2 runs Micromet 1 layup-Phenolic 1 cure cycle
2 runs Micromet 2 layup-Phenolic 2 cure cycle

The phase-gain data from the temperature ramp cycles indicate a highly conductive material and a boundary layer effect (Fig. 19). While the phase-gain response remains in the region of zero-zero (or an electric short), vacillations in the trace reveal electrical transformations in the material. The cure cycle responses vary from conductor to dielectric response. These data may be augmented by reviewing the electric response versus time curves (Fig. 20). A doublet noted in loss factor, phase, tan delta, and gain curves is displayed at ~ 40 and $\sim 60^\circ\text{C}$. This doublet is reproducible throughout the frequency range monitored, 10 to 10,000 Hz (Fig. 20). A possible inflection is noted at approximately 140°C. No attempt was made to remove volatiles from the system; these volatiles may account for the deterioration of the signal above 140°C.



A. 124/30.5 RESIN TO CATALYST (BY WEIGHT) RATIO
 B. 125/30
 C. 126/29.5
 D. GEL POINT COMPARISON OF A, B, AND C AT $\omega = 1$ K Hz.
 (1 = 100 Hz, 2 = 500, 3 = 1000 Hz, 4 = 5000 Hz, 5 = 10000 Hz.)

Figure 18. Room temperature dielectric cure monitoring of Hercules 55A resin.

TABLE 1. WATER PICK-UP DETERMINATION

PHEN1

Post-cure dielectric responses			After 1 hour at 50°C		
Frequency	ϵ'	ϵ''	Frequency	ϵ'	ϵ''
0.01	11.9	0.001	0.01	816.5	0.001
0.1	9.5	0.001	0.1	810.7	0.001
1.0	8.8	0.001	1.0	811.0	0.001
10.0	8.8	0.001	10.0	811.0	0.001
100.0	8.7	0.127	100.0	810.2	4.173
1000.0	8.9	1.266	1000.0	810.8	85.969
10000.0	8.4	4.485	10000.0	473.4	372.933

TABLE 2. CURE MONITORING OF PHENOLIC COMPOSITES

Number of Runs	Run Conditions	Event	Event Temperature	Theorized Event Significance
2	temperature ramp no vacuum 1000 psi 10, 100, 1000, 10000 Hz direct lay-up	peak	40°C	unknown, perhaps trapped volatile efflux
		peak	60°C	flow
		deterioration of signal	140°C	unknown, perhaps crosslinking catalyst scission or volatile efflux
1	full cure (new) vacuum 10, 100, 1000 10000 Hz direct lay-up	slope change	140°C	catalyst scission
		deterioration	approximately 100 minutes at 154°C	unknown; perhaps crosslinking or volatile efflux
Note: no low temperature data due to high conductivity effects				
1	full cure (new) vacuum 100, 500, 1000, 5000, 10000 Hz indirect lay-up	recovery of signal	55°C	flow
		slope change	second temperature hold*	volatile or water efflux
		slope change then deterioration	140°C	catalyst scission
		slope change	approximately 100 minutes at 254°C	unknown; perhaps gell point
		on-going deterioration of signal		unknown; perhaps due to build-up of polar moieties
3	DMA run no vacuum temperature cycles	slope change	60°C	flow
		slope change	115°C	unknown; perhaps volatile efflux
		slope change	145°C	unknown; perhaps catalyst scission or gelation

*95-105°C due to associated endotherm

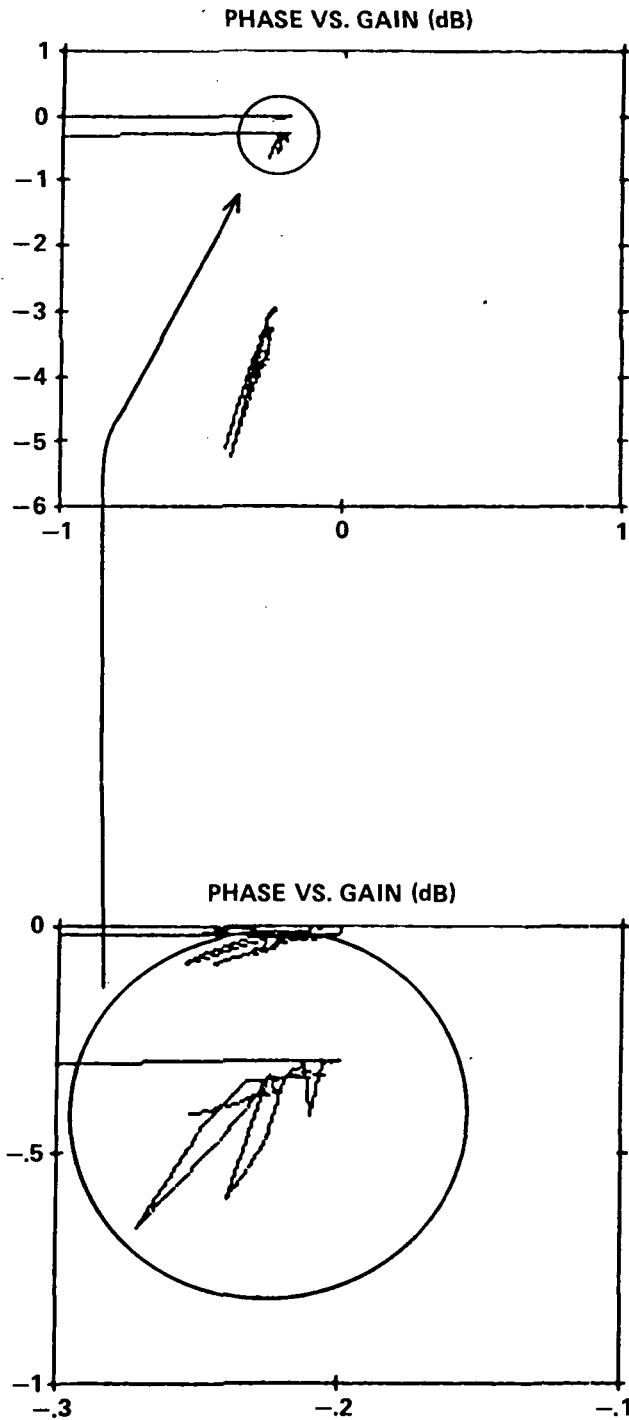
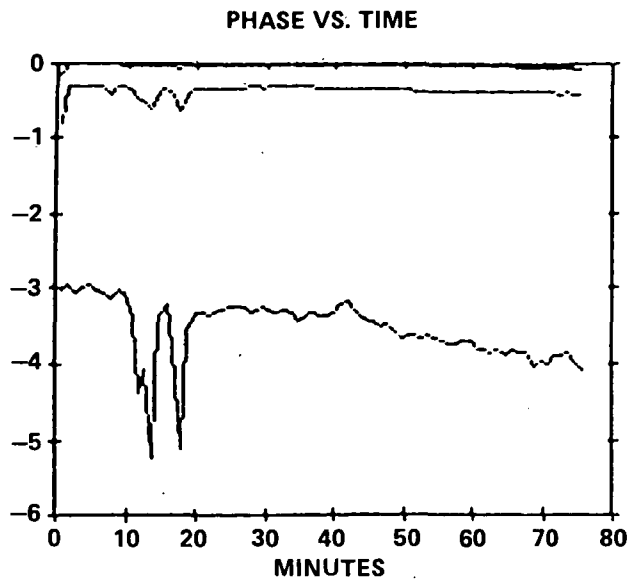
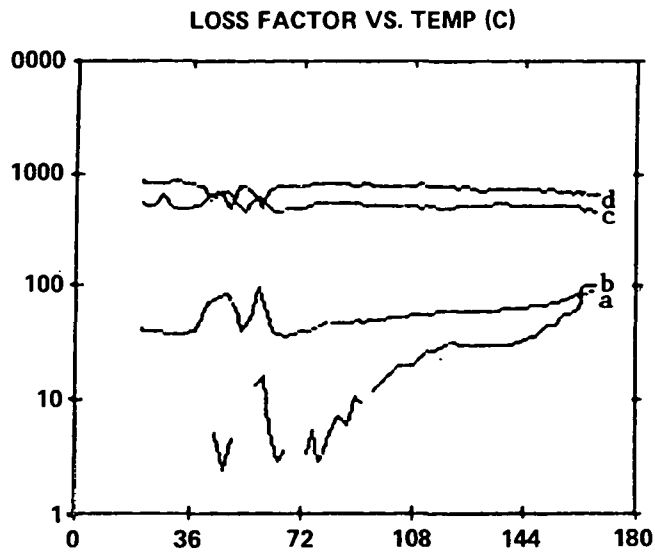


Figure 19. Highly conductive material phase versus gain responses. The blow-up region reveals that the responses of all frequencies are similar.



NOTE THE PRESENCE OF A DOUBLET AT 40° AND 60°F – 10 TO 20 MINUTES. IT APPEARS THE SIZE OF THE RESPONSE IS IN DIRECT CORRELATION TO THE FREQUENCY.

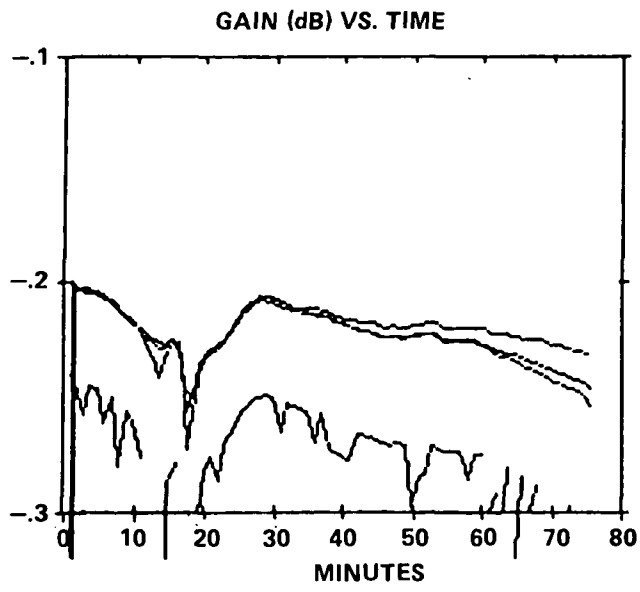
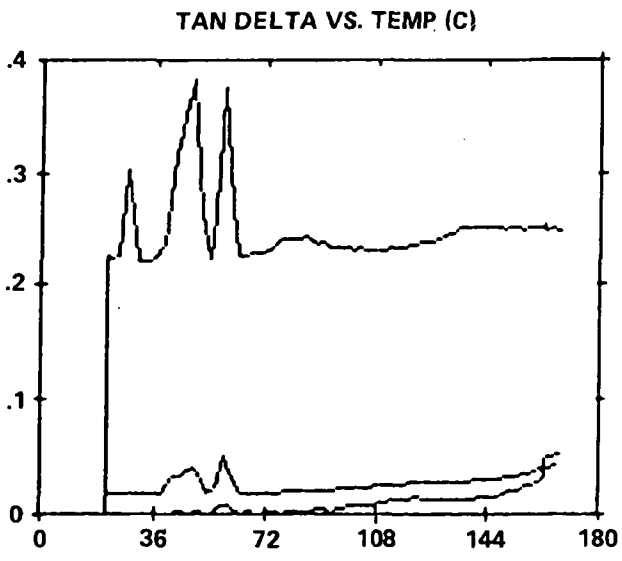
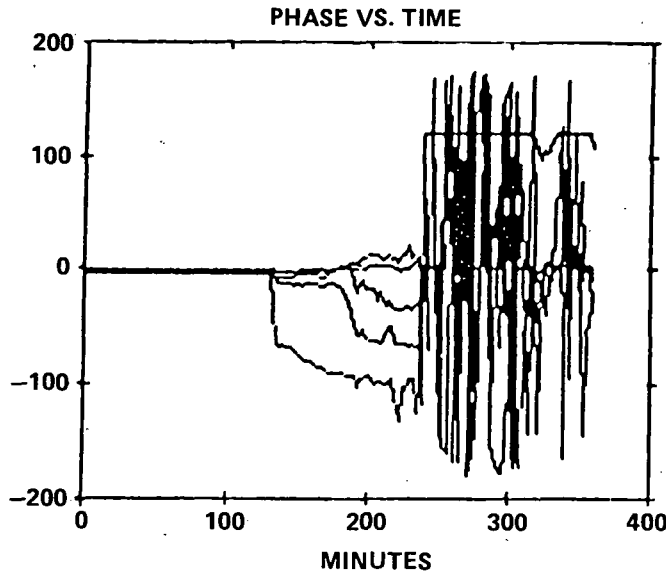


Figure 20. Dielectric responses for phenolic composite material for frequencies (a) 100, (b) 500, (c) 1000, and (d) 10000.

Two full cure cycles were monitored, under vacuum. One, a direct cure method, maintained 0 phase and gain responses to 140°C. At that point the signal deteriorated, possibly due to the water formed during cross-linking (Fig. 21).



NOTE THE TRANSITION REGION FROM APPROXIMATELY 130 TO 240 MINUTES; BEFORE THIS REGION, THE SIGNAL INDICATES HIGH CONDUCTIVITY; AFTER THIS REGION THE SIGNAL IS LOST.

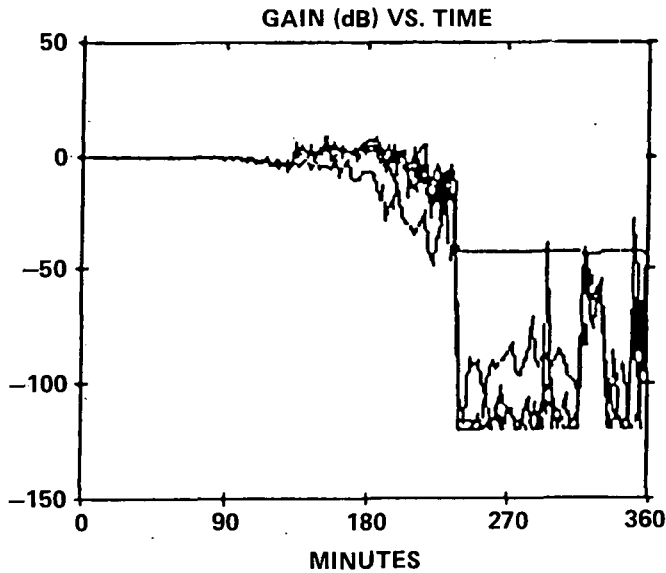


Figure 21. Phase and gain responses for a direct lay-up procedure on phenolic composite material. Note the shifts in the frequency responses in the transition region.

To correct the conductivity problems, an indirect lay-up method was attempted (Figs. 22 and 23). The onset of flow may be clearly determined at approximately 55°C. The next event occurs during the second temperature hold (95-105°C). An inflection is noted on the loss factor and permittivity curves; an endotherm is noted for the temperature display (Figs. 24, 25 and 26). As the temperature cycle is also

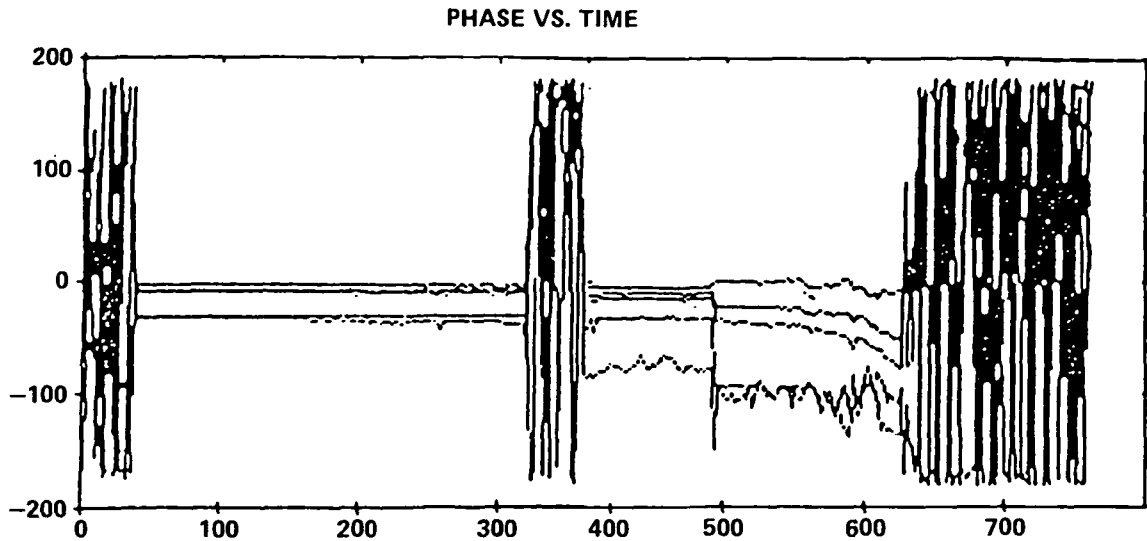


Figure 22. Phase response for indirect lay-up procedure for phenolic composite material. Note the transition regions and periods of signal loss.

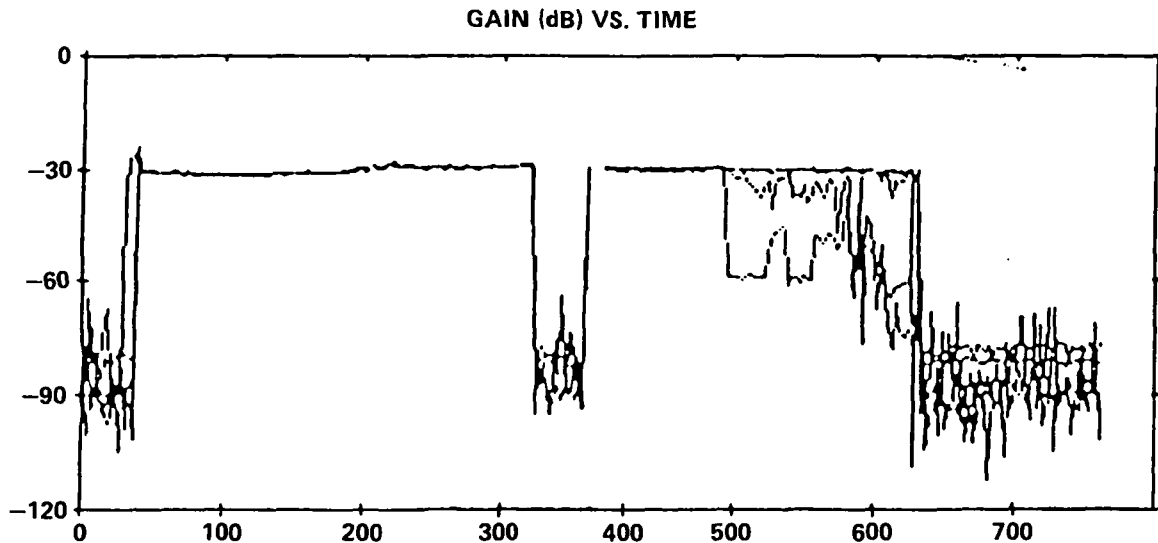


Figure 23. Gain response for indirect lay-up procedure for phenolic composite material. Note the transition regions and periods of signal deterioration for frequencies 100, 500, 1000, 5000 and 10,000 (from bottom to top respectively).

computer controlled, the in situ microchip temperature monitored is, in essence, a DTA response). This event appears tied to the boiling point of trapped volatiles.

At approximately 140°C a deviation in the dielectric responses precedes a loss of signal. This loss of signal is not displayed by the temperature cycle; the problem is not in the sensor (Figs. 22 through 26). It appears that the dielectric response is masked by the thermal activation of the catalytic agents. As the ions are removed

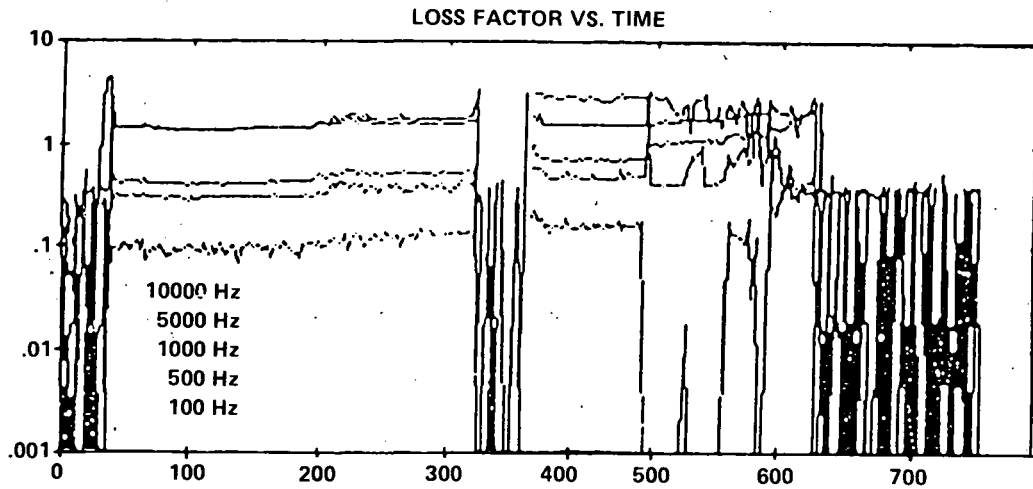


Figure 24. Loss factor response for indirect lay-up procedure for phenolic composite material.

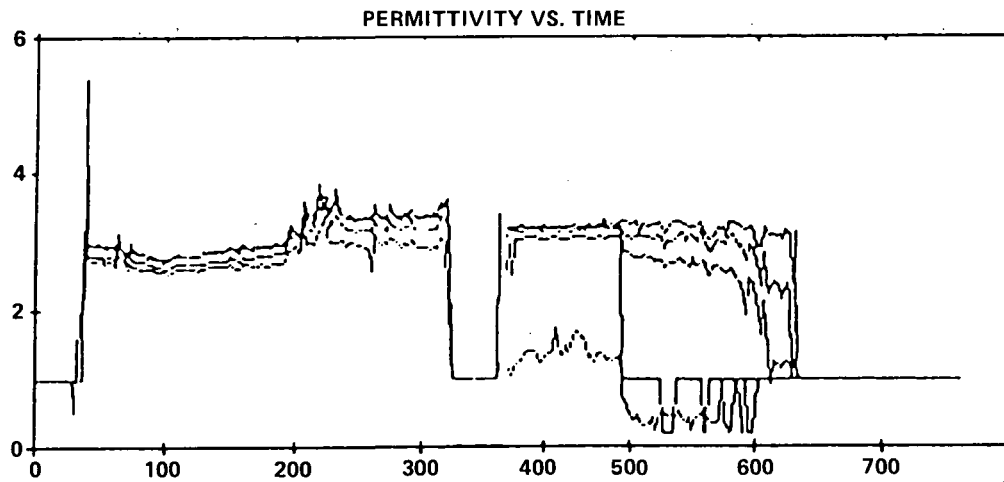


Figure 25. Permittivity response for indirect lay-up procedure for phenolic composite material.

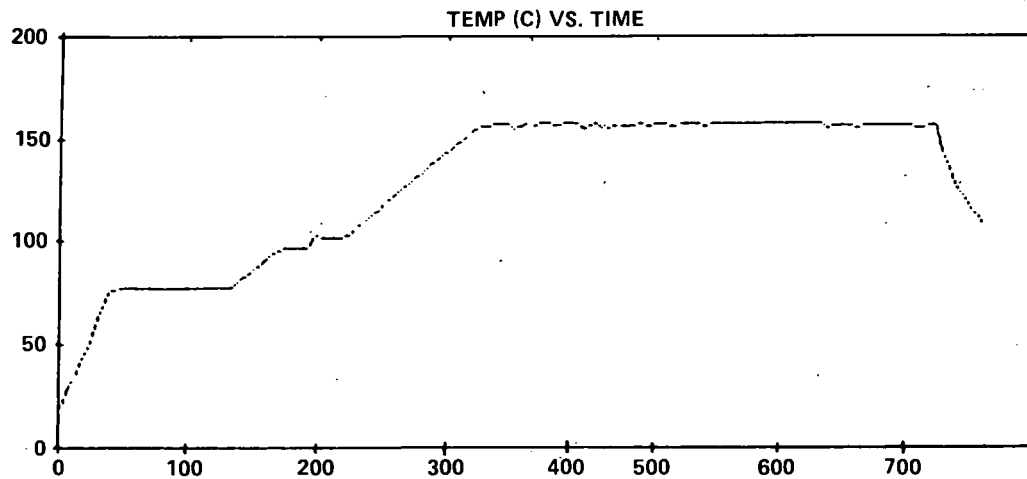


Figure 26. Temperature response for indirect lay-up procedure for phenolic composite material.

from the system during cross-linking, the signal returns. One final event is noted: a deviation of all signals approximately 100 minutes into the final temperature hold with subsequent loss of signal. This deviation may indicate the water influx during cross-linking or gellation of the system. More research is necessary to determine the exact significance of the five events. Initial corroboration of these events has been found in DMA full cure cycle monitoring; three reproducible events were noted: at 60°C, at 115°C, and at 145°C (Fig. 27).

SUMMARY

Two methods of dielectric cure monitoring have been investigated: parallel plate electrodes (Audrey) and microchip monoprobe (Micromet). While evidencing potential viability for low conductivity epoxy resin monitoring, the Audrey system with current electrodes appears to be incompatible with phenolic composite materials. Further work is necessary to determine the source of these incompatibilities: inherent Audrey limitations or electrode induced limitations.

The Micromet System II appears to be a viable means for cure monitoring of both epoxies and phenolic materials. While initial cure monitoring data for phenolic composite materials display reproducible events, further work is necessary to determine, not theorize, data significance. Further promise is added to the microprobe monitoring technique by the corroboration of dynamic mechanical analysis data. Again, further work is warranted. It must be noted that, as yet, no data exists to indicate the applicability of the Micromet System to feedback control.

Finally, an additional conductivity related term has been indicated for the dielectric permittivity, ϵ' . This term, heretofore unreported, becomes important when boundary layer effects and subsequent electrode shielding are noted. Initial investigations indicate that this term should be diffusion controlled. One possible oversimplified expression has been derived:

$$\epsilon'_{\text{ionic conduction}} = \frac{D(t)De}{vkt}$$

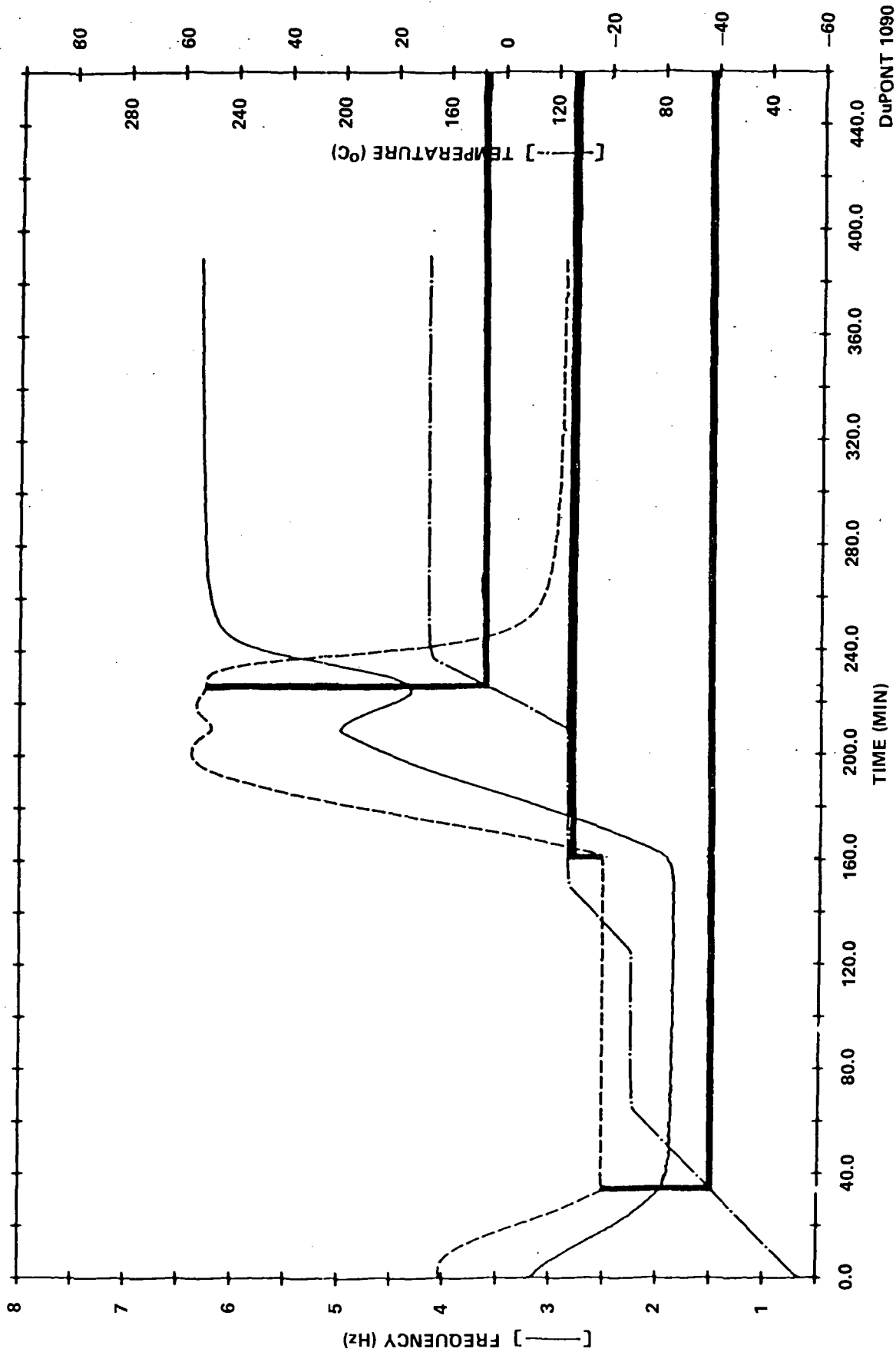


Figure 27. Dynamic mechanical testing of phenolic composite material. The dark black lines tie temperature to transition regions.

REFERENCES


1. Bottcher, C. J. F. and Bordewijk, P.: *Theory of Electric Polarization*, 2nd ed. Vol. 2, Elsevier Scientific Publishing Company, Amsterdam, 1978, p. 1.
2. Parker, T. J.: in *Polymer Science*, Vol. 2, edited by A. D. Jenkins. North Holland Publishing Company, Amsterdam, 1972, p. 1297.
3. Senturia, S. D., Sheppard, N. F. Jr., et al.: *SAMPE Journal*, July/August 1983, p. 22.
4. Reed, C. W.: in *Dielectric Properties of Polymers*, edited by F. E. Karasz. Plenum Press, New York, 1972, p. 343.
5. Bartener, G. M., and Zelerev, Y. V.: *Relaxation Phenomenon in Polymers*. John Wiley and Sons, New York, 1974, p. 25.

APPROVAL

DIELECTRIC CURE MONITORING: PRELIMINARY STUDIES

By Benjamin E. Goldberg and Marie Louise Semmel

The information in this report has been reviewed for technical content. Review of any information concerning Department of Defense or nuclear energy activities or programs has been made by the MSFC Security Classification Officer. This report, in its entirety, has been determined to be unclassified.



R. J. SCHWINGHAMER
Director, Materials and Processes Laboratory